Final Technical Report

Award # DE- SC0020982: Self-assembly of co-continuous nanostructured copolymer templates with compositional and architectural dispersity (DOE-CUB-20982)

DOE Office of Science, Basic Energy Sciences Materials Chemistry Program

PI: Ryan C. Hayward, University of Colorado Boulder
Project dates: 8/1/2021 - 1/31/2023

1. Abstract

In our previous DOE-supported project (DE-SC0016208), we demonstrated that a particular architecture dubbed ‘randomly end-linked copolymer networks’ (RECNs) led to especially robust self-assembly of disordered cocontinuous nanostructures. Such structures, wherein both microphases are fully percolating in three dimensions, are attractive for a wide-variety of energy-relevant applications including purification membranes, separators in batteries and fuel cells, catalyst supports, and high surface area electrodes. In the current project we sought to substantially extend our fundamental understanding of how different types of randomness in blocky copolymer architecture contribute to the robust formation of disordered cocontinuous nanostructures. To do so, we filled in the sizable gap between the previously studied cases of randomly linked linear multiblock copolymers and RECNs by studying two intermediate cases: (i) random miktoarm star polymers, which contain dispersity in the number of the two chemically-incompatible strands located at each junction and **therefore the preferred interfacial curvature of each polymer**, and (ii) randomly branched copolymers, which also possess bridging strands that stretch across domains **and apply local ‘elastic’ forces to the interfaces.** In addition, we studied a different network architecture, statistically crosslinked copolymer networks, that is more straightforward to prepare using chain growth polymerization methods, enabling more facile formation of cocontinuous nanostructures. Finally, we extended our approaches from model systems based on polystyrene and poly(lactic acid) to copolymer architectures containing either (i) polysulfone, an engineering polymer that provides excellent mechanical properties for membrane applications, or (ii) polyacrylonitrile, providing a convenient route to nanoporous carbon materials.

2. Accomplishments

2.1 Random miktoarm star copolymers

Previously, we have found that randomly *end*-linked copolymer networks (RECNs), formed by end-linking of two chemically-incompatible polymer strands with multi-functional linkers, showed formation of disordered cocontinuous phases across broad ranges of composition (e.g. at least 25 wt%). While seminal theoretical work previously focused on the role of random elastic forces imposed by the network architecture in frustrating long-range ordering, much remains to be understood about the factors promoting cocontinuity in such systems. In particular, we hypothesized that the dispersity in preferred interfacial curvature for each junction (due to an excess of one type of strand vs. the other) might play an important role in favoring disordered cocontinuous morphologies. To test this hypothesis, we selected the architecture of *random miktoarm star polymers* (RMSPs), since they contain an equivalent distribution of composition, and therefore preferred curvature, at each junction, but lack any elastic contributions.

To form RMSPs, as shown in Fig. 1a-b, we first obtained commercially available polystyrene (PS) and synthesized poly(D,L-lactic acid) (PLA) by ring-opening polymerization, each bearing a hydroxy group at one end. Subsequently these hydroxy groups were converted to azide groups through a post-treatment process. Both polymers had a number average molecular weight of ≈ 5 kg/mol. Copper-catalyzed azide-alkyne cycloaddition (CuAAC) reactions with tri-, tetra-, or hexa-alkyne crosslinkers were subsequently used to form stars. Size-exclusion chromatography, multi-angle light scattering, and nuclear magnetic resonance spectroscopy were used to confirm nearly quantitative coupling of azide and alkyne groups, leading to formation of almost entirely stars of the desired arm number, apart from a small fraction (≈ 5 wt. %) of residual PS homopolymer arising predominantly from chains that were not successfully end-functionalized in the original synthesis.

After solvent evaporation and annealing at 150 ºC for 1 d, microphase separation of a PS/PLA RMSP was characterized using small-angle X-ray scattering (SAXS), which revealed a disordered nanostructure with a characteristic length-scale of 22 nm (Fig 1c). By monitoring the mass loss by each sample following incubation in a basic solution that etches accessible PLA, we assessed the extent of PLA percolation. Correspondingly, by monitoring whether the SAXS pattern lost its characteristic features corresponding to nanoscale structure, and visualizing the porosity of the remaining materials via scanning electron microscopy, we assessed the extent of PS percolation.

As shown in Fig. 1d, 4-arm RMSPs exhibited a wide (25 wt. %) window of disordered cocontinuous phases, nearly as large as comparable RECNs, even though the star architecture does not give rise to random elastic forces at junctions. Interestingly, however, this behavior is highly sensitive to arm number, with 3-arm RMSPs exhibiting an ≈ 15 wt. % wide window, and 6-arm RMSPs not showing *any* measurable cocontinuous domain. We rationalized these findings in terms of the effect of homopolymer stars suppressing percolation in the former case, and in terms of the reduced distribution of preferred curvatures with increasing arm number in the latter. A manuscript describing these results is currently being prepared for submission [1].

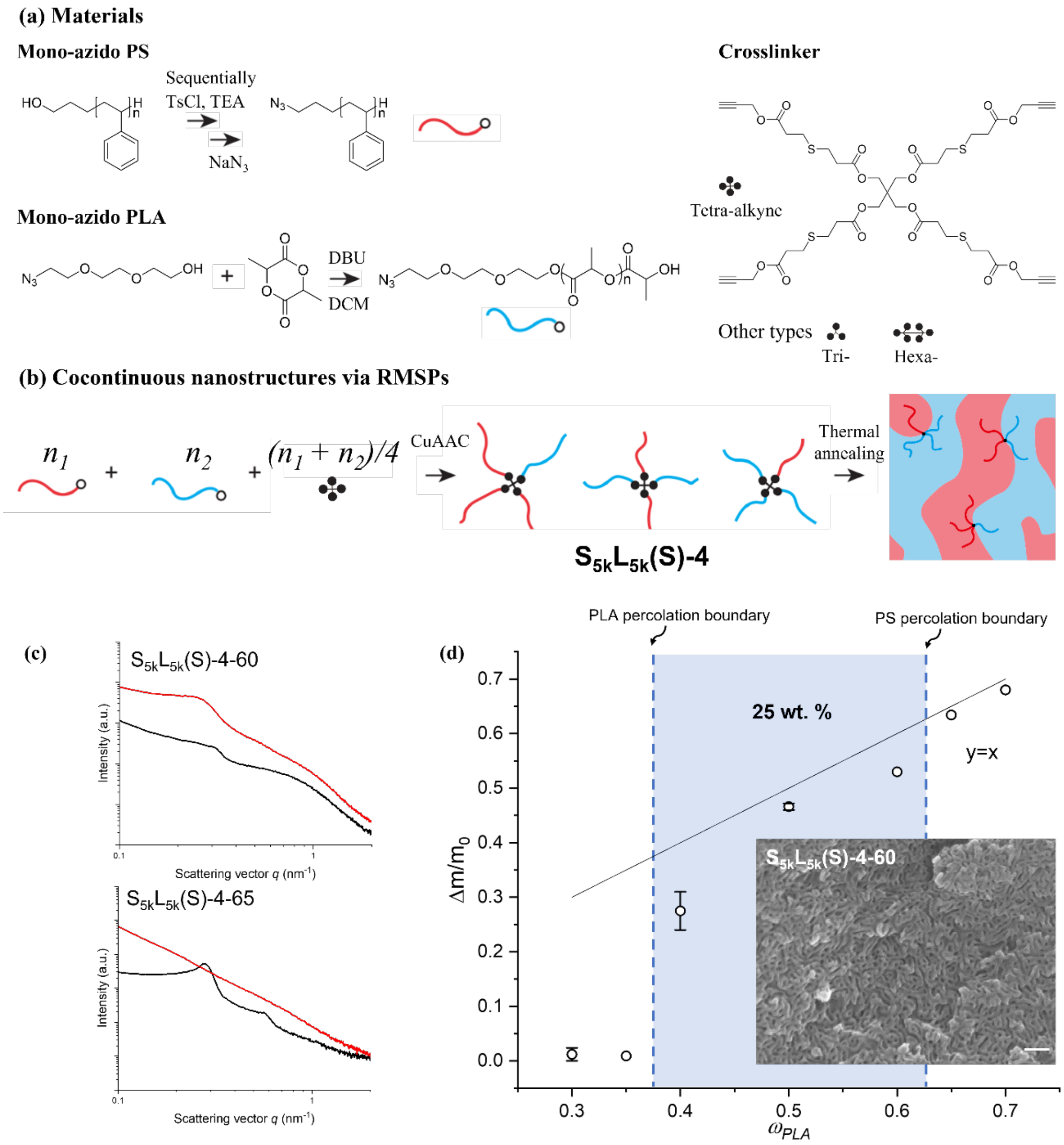

Figure 1. (a) Synthesis of RMSPs and (b) a processing schematic for the formation of cocontinuous polymeric nanomaterials using RMSPs. The 4-arm RMSPs are named as S$_{5k}$L$_{5k}$(S)-4 where the subscript 5k means the molecular weight of each polymer (5 kg/mol), S represents star, and 4 is the crosslinker functionality. (c) SAXS patterns of S$_{5k}$L$_{5k}$(S)-4-60 and S$_{5k}$L$_{5k}$(S)-4-65 before and after PLA etching (black and red), where 60 and 65 represent the weight fraction of PLA. S$_{5k}$L$_{5k}$(S)-4-60 showed a largely preserved SAXS pattern after PLA etching; while S$_{5k}$L$_{5k}$(S)-4-65 exhibited the loss of the characteristic peaks. (d) Cocontinuous window of S$_{5k}$L$_{5k}$(S)-4 defined by PLA and PS percolation from gravimetry and SAXS, respectively. The inset SEM image showed an interconnected nanoporous PS after PLA etching, supporting the defined cocontinuous window (scale bar: 100 nm).

2.2 Randomly branched copolymers

The results described in section 2.1 indicate that a distribution of preferred interfacial curvatures is *sufficient*—and therefore that the random elastic forces associated with network architectures are *not required*—to promote a wide disordered cocontinuous phase, at least in the case of 4-arm star polymers. Nevertheless, the strong sensitivity of this behavior to the junction functionality of the star polymers, suggests that elastic contributions may also be important in some cases. To bridge the gap in our understanding between RMSPs and RECNs, we next considered randomly-linked *branched* copolymers (RBCs). This architecture allows for the systematic regulation of the extent of elastic contributions arising from strands that bridge between multiple junctions by controlling the degree of branching, while also preserving the same distribution of preferred interfacial curvature present in both RMSPs and RECNs.

To form RBCs, we first obtained commercially available polystyrene (HO-PS and HO-PS-OH) and synthesized poly(D,L-lactic acid) (HO-PLA, HO-PLA-OH). Subsequently, these terminated hydroxy groups were converted to azide groups through a post-treatment process. Polymers were found to have number average molecular weights of ≈ 5 kg/mol. Copper-catalyzed azide-alkyne cycloaddition (CuAAC) reactions with tri-, tetra-, or hexa-alkyne crosslinkers were subsequently driven. The conversion was again determined to be very high, i.e., ≥ 97 %.

After solvent evaporation and annealing at 150 ºC for 1 d, microphase separation of PS/PLA RBCs was characterized using small-angle X-ray scattering (SAXS), which revealed a disordered nanostructure with a characteristic length-scale of 25 nm. As before, gravimetry and SAXS were used to determine the window of cocontinuity. We found that for each junction functionality, the breadth of the cocontinuous window increased as the degree of branching increased (as controlled by the ratio of mono- to di-functional polymer strands). Remarkably, the RBCs with tri-alkyne crosslinkers and an average end functionality of polymers (1.6) achieved a 35 wt. % cocontinuous window while maintaining solution-processability. A manuscript describing these results is currently being prepared for submission [2].

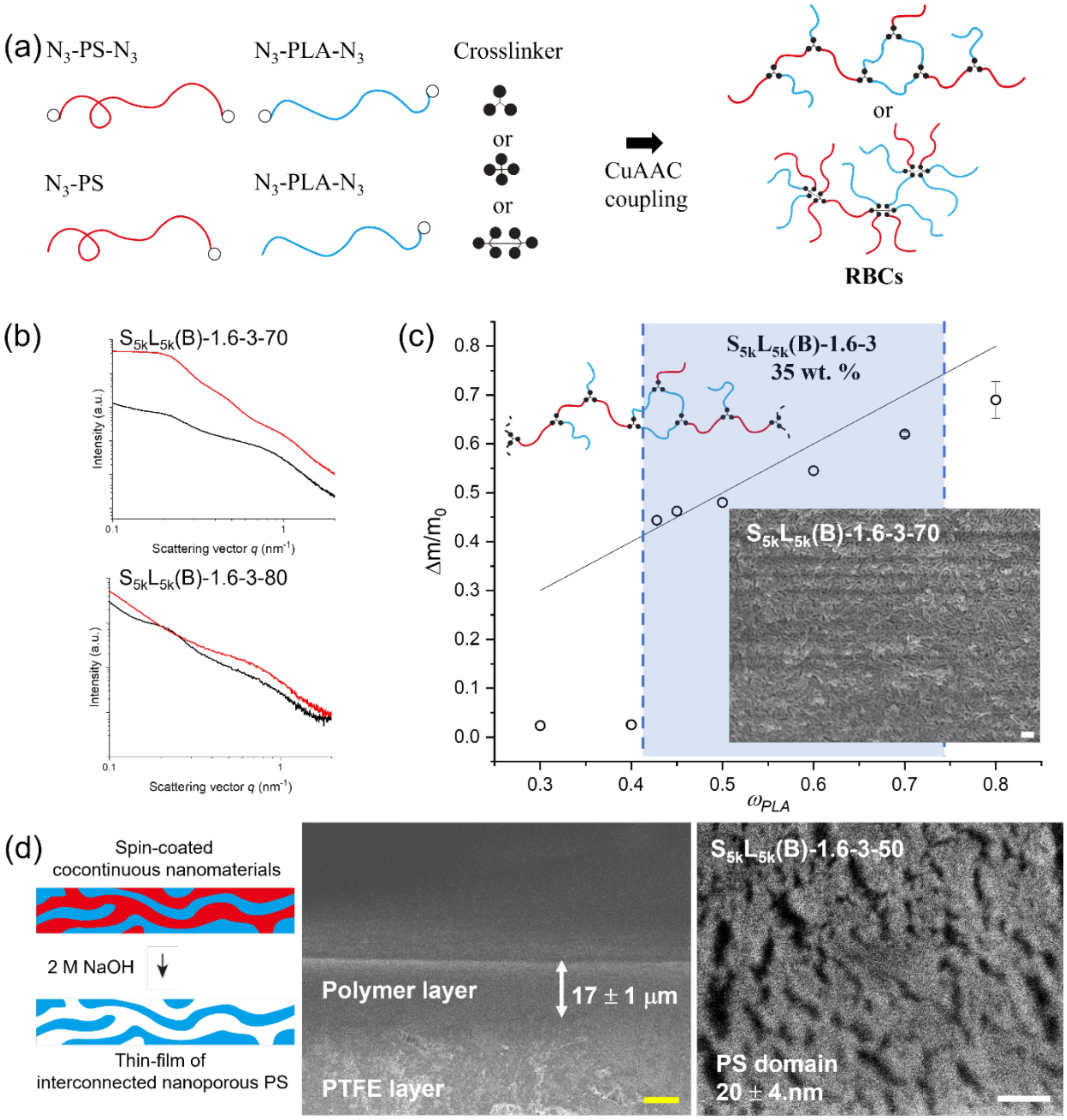

Figure 2. (a) Preparation of RBCs. (b) SAXS of $S_{5k}L_{5k}$(B)-1.6-3-70 and $S_{5k}L_{5k}$(B)-1.6-3-80 before and after PLA etching (black and red), where the subscript 5k refers to the molecular weight of both PS and PLA (5 kg/mol), B denotes branched, and the subsequent three numbers are polymer- and crosslinker functionality, and weight fraction of PLA. (c) Cocontinuous window of $S_{5k}L_{5k}$(B)-1.6-3 defined by PLA and PS percolation from gravimetry and SAXS, respectively. The inset SEM image shows an interconnected nanoporous PS at 70 % PLA. (d) A film of interconnected nanoporous PS from $S_{5k}L_{5k}$(B)-1.6-3-50 formed by solution coating and PLA etchin. White scale bars are 100 nm and yellow is 1 μm.

2.3 Statistically cross-linked copolymer networks

Much of our work prior to this project has focused on randomly *end*-linked copolymer networks (RECNs), formed by reaction of telechelic end-functional polymer chains with a multi-functional linker. While effective for formation of cocontinuous polymeric nanomaterials (CPNs), this approach requires a high degree over chain end functionality, which for chain growth polymerizations generally entails the use of a controlled ('living') polymerization, a difunctional initiator, and typically a subsequent step to convert the resulting chain ends to the desired functionality. Here we sought to understand whether similar results could be obtained using statistically *cross*-linked copolymer networks (SCCNs); these can be formed by preparing linear polymers containing a small fraction of readily cross-linkable comonomers, meaning that each of the above limitations can in general be avoided.

To form SCCNs, we first synthesized polystyrene (PS) and poly(2-vinylpyridine) (P2VP) copolymers, each bearing several mole percent of allyl methacrylate, by RAFT copolymerization (Fig. 1). The pendent allyl functional groups do not participate to significant extent in the radical polymerization, but can subsequently be reacted with multi-functional thiols to form SCCNs. Polymers were found to have number average molecular weights of ≈ 25 kg/mol, with average number of allyl groups per chain (f_p) of 4 - 6. Thiol-ene reactions with tri-, tetra-, or hexa-thiol crosslinkers were subsequently driven using a UV photoinitiator. The conversion was monitored by FT-IR (Fig. 2a), wherein the nearly complete disappearance of peaks at 2550 cm^{-1} (S-H stretch) and 1640 cm^{-1} (C=C stretch) indicated essentially quantitative conversion.

Following solvent evaporation and annealing at 180 °C for 1 d, small-angle X-ray scattering (SAXS) was employed (Fig. 2b) to characterize microphase separation of a typical PS/P2VP SCCN. One broad peak centered at 0.011 Å^{-1} can be observed, indicating a disordered nanostructure with a characteristic length-scale of 50 nm. Subsequent washing with 2 M NaOH in a 1:1 (vol.) mixture of water and methanol was used to cleave the ester groups in the crosslinker and extract the P2VP component. Notably, the SAXS peak does not shift in location but increases in intensity, indicating that the structure of the PS domains does not change substantially during P2VP removal. Visualization of the self-assembled morphology was carried out with TEM and SEM. TEM images (Fig. 2c, P2VP domains are dark due to staining with iodine) clearly reveals a disordered structure, which appears to be cocontinuous. Similarly, SEM images (Fig. 2d) after etching are consistent with a nanoporous PS structure with interconnected pores. The average size of the PS domains in both cases is 30-35 nm, similar to that expected from the SAXS measurements and the PS content (50 wt. %)

As the number of allyl pendants per polymer chain increased, a decrease in domain spacing was observed. While the SCCNs with f_p = 4.2 had almost the same domain spacing (≈ 50 nm) despite variations in crosslinker functionality, the characteristic peak of the SCCN with f_p = 5.7 showed a smaller domain spacing (32 nm). This difference in domain spacing based on f_p can be attributed to the shorter chain length between crosslinkers in the SCCN with f_p = 5.7 compared to the other SCCNs with f_p = 4.2. A manuscript describing these results is currently being prepared for submission [3].

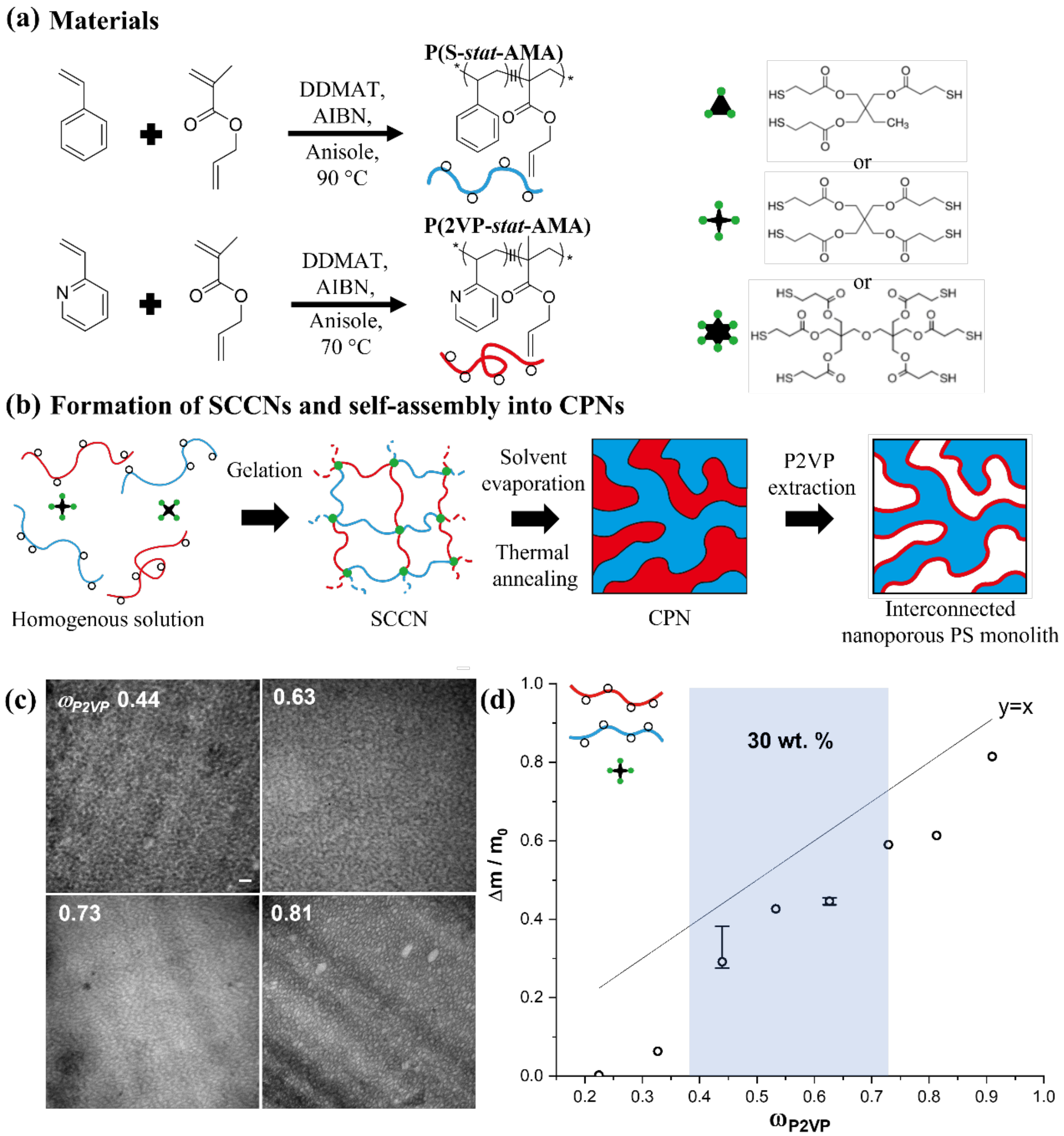

Figure 3. (a) Statistical copolymers and crosslinkers used to construct SCCNs. (b) Processing schematic for the formation of CPNs and interconnected nanoporous materials. (c) TEM images of $S_{25k}2VP_{28k}$-4.2-4-ω_{P2VP} after I_2-staining on P2VP, where the subscript 25k and 28k mean the molecular weight of PS and P2VP (25 and 28 kg/mol), respectively, and the following two numbers represent the allyl number per chain and crosslinker functionality. $S_{25k}2VP_{28k}$-4.2-4-0.81 showed dispersed P2VP domains in a matrix of PS, while the other three displayed cocontinuous phases. (scale bar: 100 nm) (d) Cocontinuous window of $S_{25k}2VP_{28k}$-4.2-4 defined by P2VP and PS percolation from gravimetry and SAXS, respectively, showing a wide cocontinuous range (30 wt. %), comparable to that of RECNs.

2.4 Polysulfone-based random copolymer architectures

While most of our work to date has focused on model systems constructed from PS and PLA strands, the brittle nature of PS (especially the low molecular weight strands we have used) means that the nanoporous materials prepared upon etching of PLA are far too fragile for use in any applications. Thus, we sought to replace PS with the engineering polymer polysulfone (PSU). After etching of the poly(lactic acid) (PLA) component, the resulting porous PSU materials have sufficient mechanical robustness to serve as, e.g., separation membranes.

RECNs formed from telechelic PSU and PLA strands with a tetrafunctional crosslinker were found to have a broad cocontinuous window and superior stiffness and toughness compared to PS-based RECNS (Fig. 4a-c). As a facile route to prepare solution-processable polymers that robustly form cocontinuous nanostructures, we also synthesized random linear multiblock polymers (RLMBs) using a di-thiol chain extender. Thin films for ultrafiltration were prepared by spin-coating a solution of RLMBs onto a water-filled microporous polyether sulfone (PES) membranes with a pore size of ~ 100 nm as a support. This approach resulted in a RLMB film with thickness of 200 nm as measured by TEM. Following etching of the PLA phase, the resulting nanoporous membrane showed ≈ 100 % rejection of 50 nm Au particles, with only a slight decrease in overall permeability compared to the PES supporting membrane itself. A manuscript describing these results is currently being prepared for submission [4].

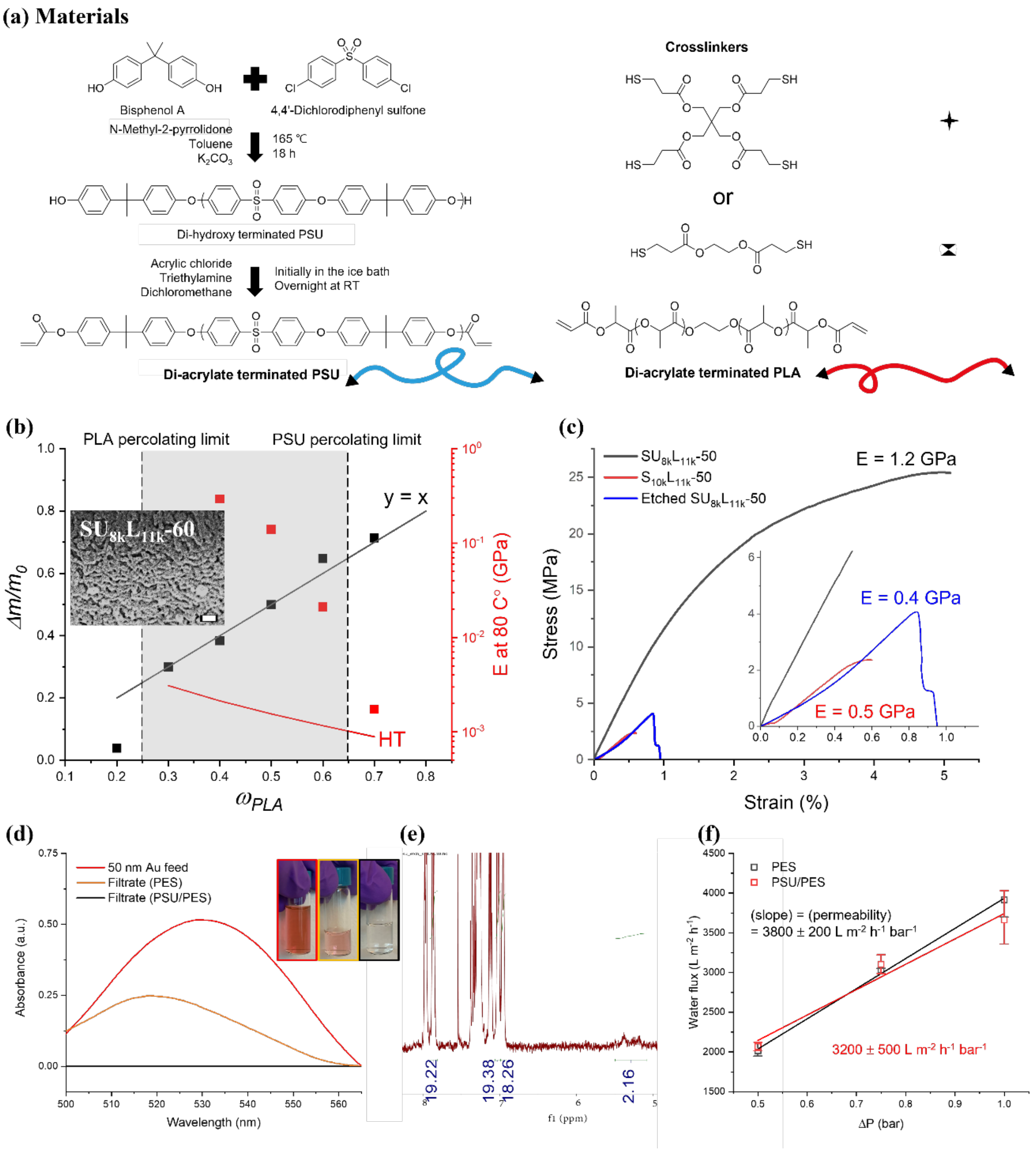

Figure 4. (a) Polymers and crosslinker/chain extender used for RECNs and RLMBs. (b) Cocontinuous window of SU$_{8k}$L$_{11k}$ RECNs defined by gravimetry and Young's modulus (*E*) measurement at 80 °C, respectively, where the subscript 8k and 11k represent the molecular weight of PSU and PLA (8 and 11 kg/mol), respectively. The inset SEM image shows an interconnected nanoporous PSU made from an RLMB with 60 wt. % PLA (scale bar: 100 nm). (c) Tensile tests of SU$_{8k}$L$_{11k}$-50 RECN, S$_{10k}$L$_{11k}$-50 RECN, and the etched SU$_{8k}$L$_{11k}$-50 RECN. (d) Separation performance of the interconnected nanoporous PSU as an ultrafiltration membrane. (e) NMR spectrum of the thin-layer interconnected nanoporous PSU, showing that 93 wt. % of PLA was etched due to PLA percolation. (f) Water permeability of the PES support and PSU/PES dual membrane.

2.5 Polyacrylonitrile-based random copolymer architectures

Nanoporous carbon structures have considerable potential in a variety of energy storage applications including supercapacitors and batteries. High surface area materials with a large fraction of available pores are desirable for operation of electrodes that are not limited by diffusion of chemical species. In addition, heteroatom dopants like nitrogen have been shown to improve the electric properties of graphitic carbon materials. Here, we sought to develop nitrogen-doped nanoporous carbons using RECNs based on polyacrylonitrile (PAN), a well-known precursor to carbon with pyridinic functionalities. While many routes to porous carbons exist, the RECN platform provides broad tunability of pore size and volume fraction through simple adjustments to strand molecular weight and volume fraction, respectively.

Our approach begins with the formation of a cocontinuous polystyrene (PS)/polyacrylonitrile (PAN) RECN. A subsequent thermal treatment at 250 - 300 °C removes the PS template phase while stabilizing PAN, followed by carbonization at 800 - 1000 °C to generate highly interconnected nanopores. Specifically, telechelic PS and PAN are polymerized via atom transfer radical polymerization (ATRP) or single electron transfer living radical polymerization (SET-LRP). We employ a di-functional initiator, leading to a high degree of bromine end-functionality, which can be changed to an azide with high conversion. These polymers can then by end-linked into a network using copper-azide alkyne chemistry (CuAAC) (Fig. 5).

Via SET-LRP synthesis we have prepared telechelic bromine-functionalized PAN with molecular weights of $\approx$ 10 kg/mol (SEC). Similarly, polystyrene synthesis by ATRP has yielded end-functional samples with molecular weights of $\approx$ 10 kg/mol. These strands have been used for successful formation of RECNs with weight fractions ranging from 40-60% PAN. FTIR results indicate a high degree of conversion of the end-linking chemistry, while SAXS measurements have suggested disordered microphase separation. The microphase separated networks are thermally treated to stabilize the structure and then carbonized. The resultant monolithic carbons demonstrate viable mechanical properties for use in a device and a high ($\approx$ 10%) pyridinic/pyrrolic nitrogen content from XPS measurements. A manuscript describing these results is currently being prepared for submission [5].

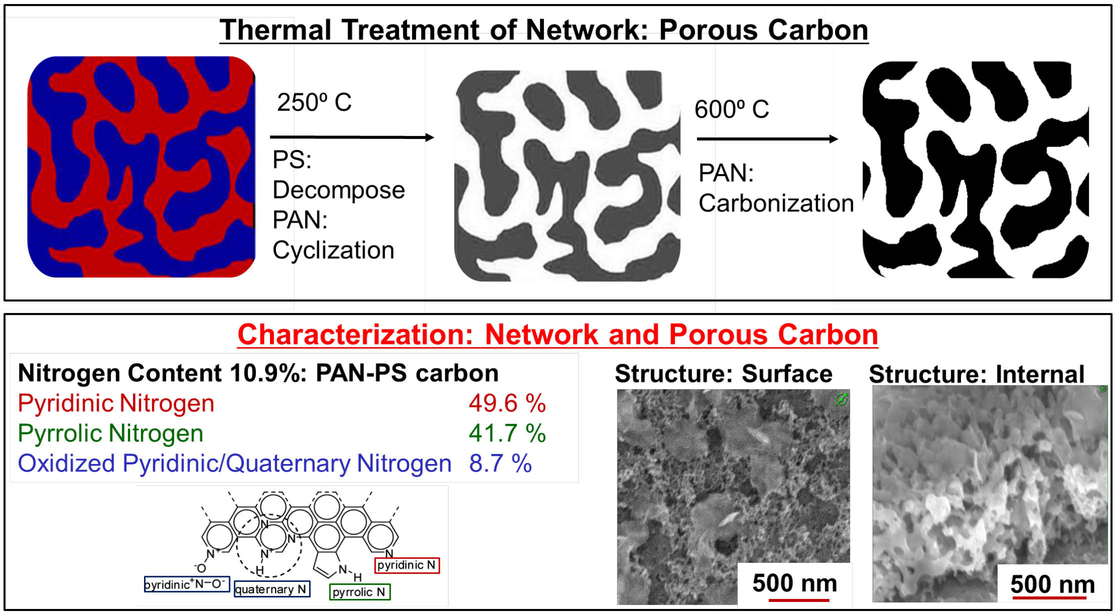

Nitrogen Content 10.9%: PAN-PS carbon	
Pyridinic Nitrogen	49.6 %
Pyrrolic Nitrogen	41.7 %
Oxidized Pyridinic/Quaternary Nitrogen	8.7 %

Figure 5. (top) Schematic illustration of two-stage thermal treatment of PS/PAN RECNs to yield nanoporous carbon. (bottom) Characterization of porous carbon by XPS and SEM.

References

[1] J. Ju, R.C. Hayward, “Random Miktoarm Star Polymers to Elucidate the Role of Dispersity of Preferred Interfacial Curvature in Stabilizing Disordered Cocontinuous Nanostructures”, *manuscript in preparation* (2023).

[2] J. Ju, R.C. Hayward, “Randomly Branched Copolymers Reveal the Contribution of Bridging Strands to Formation of Disordered Cocontinuous Nanostructures”, *manuscript in preparation* (2023).

[3] J. Ju, R.C. Hayward, “Formation of Disordered Cocontinuous Nanostructures by Statistically Crosslinked Polystyrene/Poly(2-vinyl pyridine) Networks”, *manuscript in preparation* (2023).

[4] J. Ju, R.C. Hayward, “Interconnected Nanoporous Polysulfone from Microphase Separated Networks and Disperse Block Copolymers”, *manuscript in preparation* (2023).

[5] M. Ticknor, R.C. Hayward, “Nanoporous Nitrogen-doped Carbon Derived from Polystyrene-Polyacrylonitrile Copolymer Networks”, *manuscript in preparation* (2023).